THE SIMULATION OF LASER BEAM WELDING OF SILICA ELEMENTS

Michael Göbel[1], Jörg Hildebrand[2] and **Frank Werner[3]**

ABSTRACT

The laser beam welding of silica represents an innovative alternative to traditional oxyacetylene welding. The application of this technology allows an economic bonding of silica components, which raises the standards of joint qualities to a new level.

In a research project, the Bauhaus-Universität Weimar analyzes the CO_2-laser beam welding of silica elements numerically and experimentally in co-operation with different industry partners. The development of a ready to market and effective procedure of the laser beam welding of silica is the mayor goal of the project, under use of experimental results and utilisation of highly modern numerical calculation models. Thereby, an extensive pool of experience can be accessed in the field of welding process simulation of metals. In co-operation with the Institute of Joining Technology and Materials Testing gGmbH, experimental weldings with different laser adjustments and silica plate thicknesses were carried out.

The numerical simulation uses a three-dimensional model, which also includes physical nonlinearity. Therefore, the specialised FEM software SYSWELD® is used.

KEY WORDS

CO_2-laser beam welding, silica, numerical physical nonlinear simulation, temperature dependent material properties, SYSWELD®

INTRODUCTION

The systematic evolution of an effective and economical procedure of the laser beam welding of silica is the scope of this work. In the first step, the realisation of tests is required in order to obtain experimental results. These data allow in a consecutive step a calibration of the applied calculation model, as well as the material properties. Subsequently, it is possible to find statements about the consequences of different welding parameters by using a numerical simulation. This procedure allows the calculation of optimal welding parameters to obtain the best possible welding results. Laser beam welding has the potential to be used in various fields. Examples will be applied to the welding of silica plates, silica tubes, as well as other industrial silica components.

[1] Civil Engineer, Bauhaus-Universität Weimar, Dept. of Steel Structure, Marienstrasse 5, 99423 Weimar, Germany, Phone +49 3643/58-4448, FAX +49 3643/58-4441, michael.goebel@bauing.uni-weimar.de
[2] Civil Engineer, joerg.hildebrand@bauing.uni-weimar.de
[3] Professor, frank.werner@bauing.uni-weimar.de

EXPERIMENTAL WELDINGS

In co-operation with the Institute of Joining Technology and Materials Testing gGmbH, two experiments of butt joints were realised at 2 mm, respectively 6 mm thick silica plates (figure 1). For the verification of the numerical results, transient measurements of the temperature were made during welding at a total of five points on the upper and lower side of the silica elements. The temperature was measured with thermocouples (0,08 mm wire sizes) with a frequency of 100 Hz. In the first series of experiments, the welding velocity was 3 mm/s with a total power of the laser beam of 670 W. In these experiments two silica plates l x b x h = 41 x 15 x 2 [mm] were butt-welded. In a second experiment silica plates with dimensions of l x b x h = 75 x 24,5 x 6 [mm] were welded (see figure 1). The total laser beam power was 508 W and the welding velocity varied between 0,3 mm/s and 0,4 mm/s.

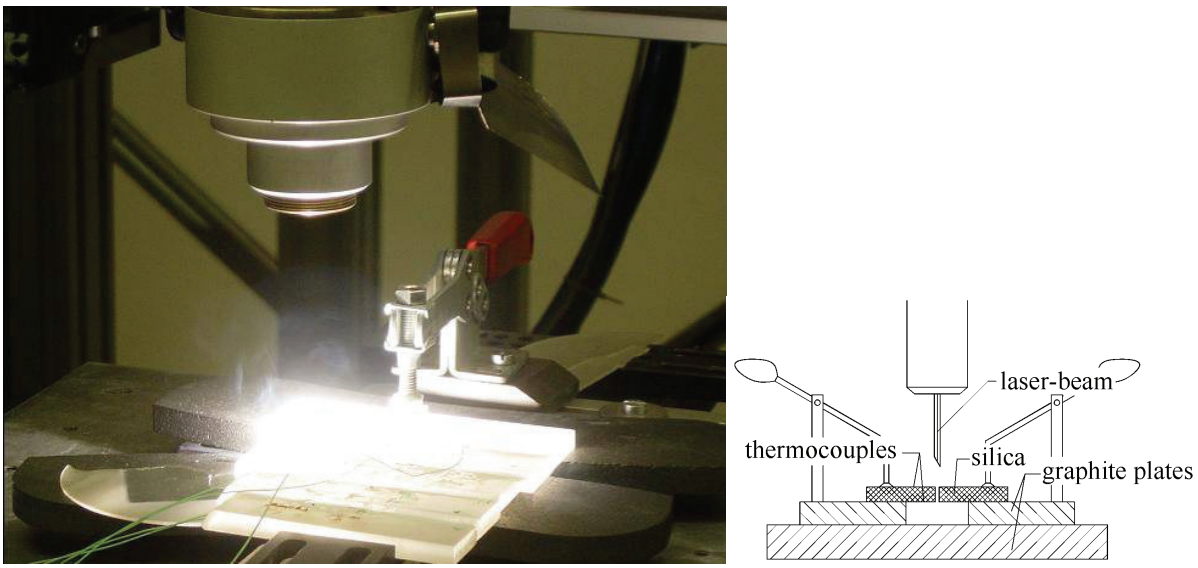

Figure 1: Experimental setup during laser beam welding of silica plates

NUMERICAL SIMULATION

BASICS

To achieve a numerical illustration of the thermal and mechanical processes that take place inside the silica during the welding process, different types of meshes were used. A compromise had to be found between required CPU time and the result accuracy of the simulation. Some examples of meshed silica components are shown in figure 2.

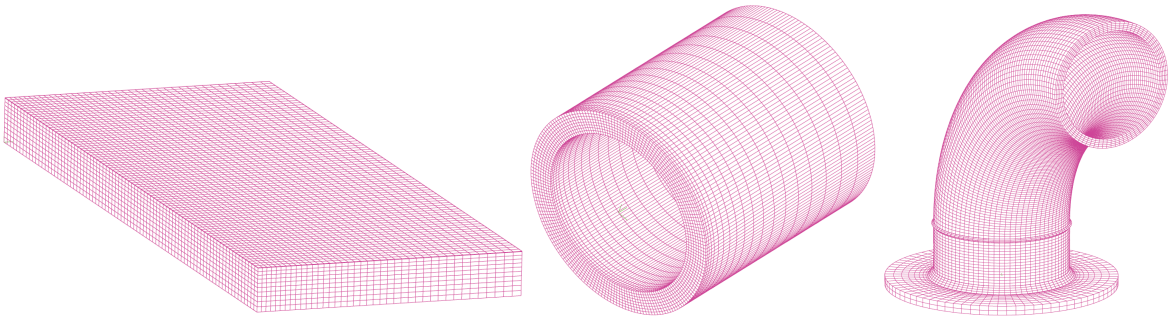

Figure 2: Meshes for different applications (left: butt welded silica plate, middle: butt welded silica tube and right: multi welded silica manifold)

During the welding process, the silica passes a temperature range from room temperature (20 °C) to a defined softening temperature of about 1750 °C and above. At this stage, it is necessary to use temperature dependent material properties in the simulation. Therefore, the numerical simulation was carried out physical non-linear. A selection of the most important material properties in dependence of temperature is illustrated in figure 3.

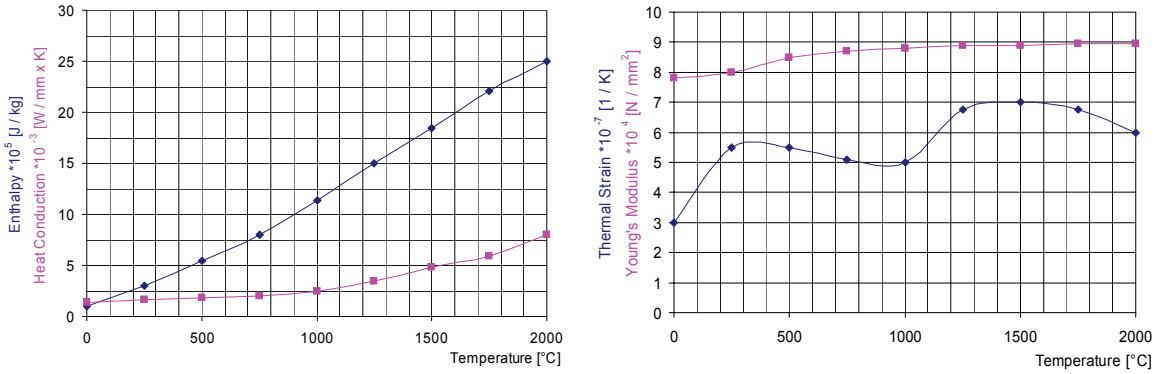

Figure 3: Temperature dependent material properties of silica: Enthalpy and Heat Conduction (left), Thermal Strain and Young's Modulus (right)

A special mechanical feature of the silica is its viscous flow behaviour. At room temperature, the silica shows an ideal elastic behaviour. When reaching the stress limit, a brittle fracture occurs. In the region of the vitreous transition temperature at 1250 °C, the reduced viscosity of the material leads to a viscous flow behaviour by which stresses are reduced.

APPLICATION OF ENERGY AND ABSORPTION

During the absorption of electro-magnetic radiation, a part of the radiation is converted into heat energy. The part of radiation that is not absorbed, is transmitted. This leads to a qualitative change of the frequency spectrum of the transmitted radiation compared to the emitted laser radiation. The absorption process depends on many factors, such as surface quality, wavelength and temperature. During the contact of the laser beam with the silica surface, the absorption rate is approximately 75 – 78 %. The wavelength of a CO_2-laser beam is

λ = 10,6 µm. In the infrared range above the wavelength of five µm, the silica is nearly opaque. According to Geotti-Bianchini et al., (1991) the radiation of the CO_2-laser is absorbed with an absorption coefficient of $\beta > 10^3$ cm^{-1}. The optical penetration of the laser is defined as:

$$\delta_{opt} = \frac{1}{\beta} \tag{1}$$

For an absorption coefficient of $\beta > 10^3$ cm^{-1} the optical penetration is less than 10 µm. The radiation intensity of the laser without optical correction is assumed mathematically idealised as GAUSSian distribution. Provided that the intensity of the laser beam is described axial symmetrical GAUSSian distributed, the following equation is applied to describe the Basic mode TEM_∞ :

$$I(r) = I_0 \times \exp\left(-\frac{r^2}{R_L^2}\right) \tag{2}$$

With I_0 : intensity on the axis (r = 0) and R_L : laser beam radius.
According to equation (2), the intensity of the laser at the beam radius decreases to approximately 37 % of the maximum level-intensity.

LOSSES THROUGH CONVECTION AND RADIATION

The specific radiation of a body is proportional to the forth potency of the absolute temperature of the black body. Under the assumption that the welding of a small part occurs in a large space, the following equation is imperative:

$$q_e = \varepsilon \times C_S \times \left\{\left(\frac{T_1}{100}\right)^4 - \left(\frac{T_2}{100}\right)^4\right\} \tag{3}$$

With ε: emission ratio, C_s: radiation constant factor of a black body in W / m^2 x K^4, T_1: temperature of the part in K and T_2: ambient air temperature in K.

The emission ratio of float glass is specified in Hohmann und Setzer (1997), at 20 °C by ε = 0,91. In addition to the radiation losses, a loss of energy arises from convection. These losses are proportional to the temperature difference between the silica surface and the air. This leads to:

$$Q_k = \dot{m} \times c_p \times (\upsilon_1 - \upsilon_2) \tag{4}$$

With $\dot{m}$: mass flow, c_p: specific heat capacity, $\upsilon_1 - \upsilon_2$: temperature difference

MECHANICAL CALCULATION MODELS (RHEOLOGICAL MODELS)

The model of Maxwell is a simple rheological model that represents the viscoplastic behaviour of silica above the vitreous transition temperature adequately. It consists of a linear elastic and linear viscous element connected in series. This configuration is represented in figure 4.

Figure 4: MAXWELL Model

The creep property is described by MAXWELL through:

$$\varepsilon(t) = \frac{\sigma_0}{E} + \frac{\sigma_0}{\eta} \times t = \sigma_0 \left[\frac{1}{\eta} \times \left(t + \frac{\eta}{E} \right) \right] = \sigma_0 \times D(t) \,. \tag{5}$$

With ε: strain, σ: stress, E: Young's modulus, η: dynamic viscosity, t: time, D: creep yield

The relaxation behaviour is expressed by:

$$\sigma(t) = \varepsilon_0 \times E \times e^{-\left(\frac{E}{\eta} \times t\right)} \tag{6}$$

The STANDARD SOLID Model represents an expansion of the model according to MAXWELL Christensen (1982). It describes the relation between the ultimate Young's modulus E_∞, the time dependent Young's modulus E(t) and the dynamic viscosity η. This model represents the mechanical behaviour of silica below vitreous transition temperature at small displacements and strains. The mechanical material behaviour of a visco-elastic solid body is schematically illustrated in figure 5.

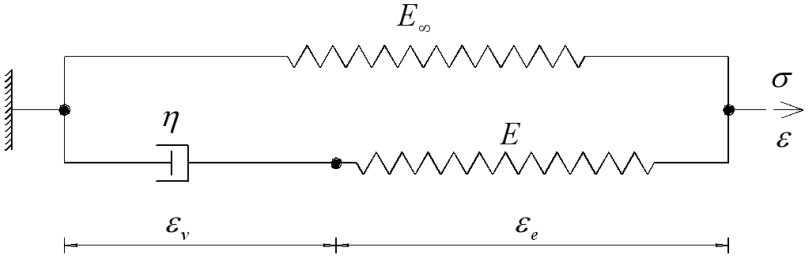

Figure 5: Viscoelastic Solid Model (ZENER Model, MAXWELL type)

The time-dependent Young's modulus E(t) can be described by the following equation:

$$E(t) = E_\infty + E \times e^{-\left(\frac{E}{\eta} \times t\right)} \tag{7}$$

The stress-stain behaviour of a viscoelastic solid can be expressed as follows:

$$\sigma = \sigma_\infty + \sigma_{ve} = E_\infty \times \varepsilon + \eta \times \dot{\varepsilon}_v \tag{8}$$

This model represents the viscoelastic solid behaviour of the silica below the vitreous transition temperature well. Above the vitreous transition temperature, the viscoplastic influence increases strongly in the material behaviour. For a better representation of the viscoplastic behaviour in this temperature range the use of the MAXWELL model is preferable.

LASER BEAM WELDING OF A SILICA PLATE

For experimental welding of silica plates, the thermal and mechanical processes were simulated within silica plates of 6 mm thickness. The welding velocity was 0,3 mm/s. The welding has been carried out with two independent laser beams. A laser beam with low energy density and a large laser beam radius was used for the pre-heating of the silica. The second laser beam with high energy density was inserted into the gap between the silica plates as a concentrated beam with a small radius. Thereby, a depth effect was generated. Specific optics for the regulation of the energy density were not available. The energy density distribution of the laser beam was assumed as GAUSSian distributed. The total laser power was 507,3 W (preheat laser beam 427 W, concentrated laser beam 81,3 W).

THERMAL PROCESSES

The comparison between measured and computed temperature-time sequences allows a verification of the numerical results. In order to do so, two points, one on the top and one on the bottom of the silica plate, have been chosen. The position of these selected points is shown in the cross section of the silica plate in figure 6.

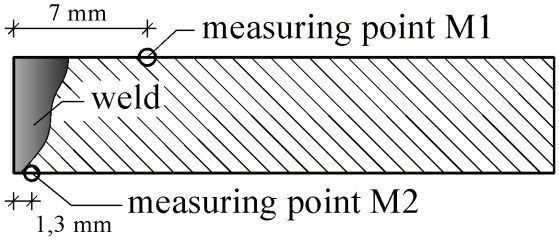

Figure 6: Cross section of the joint with measuring points

The simulation has been carried out with different assumptions for the heat source. A list of these input variables is given in table 1.

Table 1: Parameters of heat sources for different simulations

Parameters of Heat source	**SIM 1**	**SIM 2**	**SIM 3**	**SIM 4**	**SIM 5**
effective output of the preheat laser beam [W]	-	-	42,7	42,7	25,6
effective output of the focused laser beam [W]	65,1	65,1	81,3	32,5	32,5
Total Power [W]	**65,1**	**65,1**	**124**	**75,2**	**58,1**

For the effect of the concentrated laser beam, an energy input along the full weld depth has been assumed in the calculation. The intensity of the laser power decreases linearly along the depth. In figure 7 the results of the thermal calculation of the transient temperature development are represented for the measurement points, as shown in figure 6.

For simulation Nr. 5, a good analogy between experimentally obtained test data and the result of the thermal calculation could be achieved. The temperature field in the joint during the welding process is represented in figure 8 on the left side.

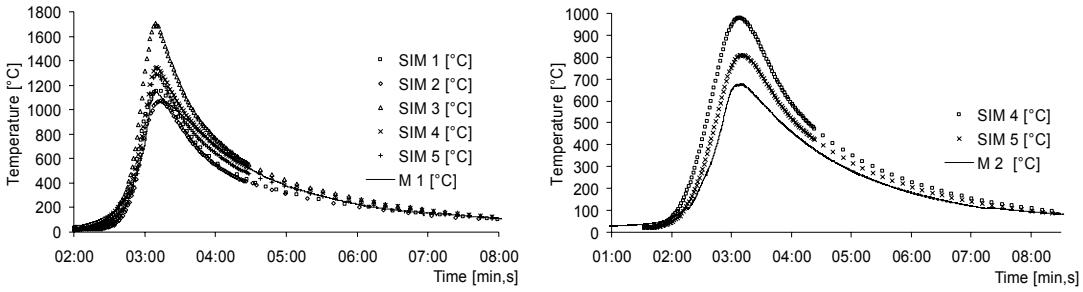

Figure 7: Temperature time diagram, experiment and simulation (points M1 and M2)

The temperature difference between the upper and lower side of the molten pool is approximately 900 °K. This leads to a big difference of the viscosities of the silica between upper and lower surface of the weld. Thus, negative effects on the quality of the joint occur. According to this, an optimization of the welding process is sensible. A possible alternative is the use of a combined welding procedure with simultaneous laser beams on the top and the bottom of the joint. The related possible temperature field is represented in figure 8 on the right.

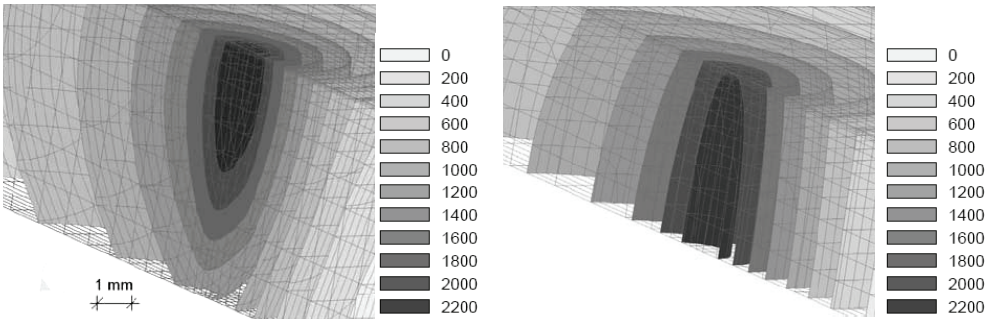

Figure 8: Image of the spatial temperature field in the joint during welding [°C]
(left: single sided welding, right: double sided welding from the top to the middle of the plate)

The use of a double-sided welding process reduces the temperature difference in the weld. This leads to an improved flow behaviour within the molten pool and allows an improvement of the joint quality.

MECHANICAL PROCESSES

The mechanical calculation follows the calculation of the transient temperature field to estimate the stress distribution during the welding process. The thermal calculation model from simulation 5 calibrated before is used for this purpose (figure 8 on the left). The here discussed analysis is limited to the axial stress σ_x normal to the joint plane.

Simulation with Standard Solid Model

The realisation of a transient physical non-linear calculation permits statements about the time-controlled stress evolution.

During the cooling process, tensile or compressive stresses are generated in fields that were loaded with viscoelastic strains during the welding process (figure 9).

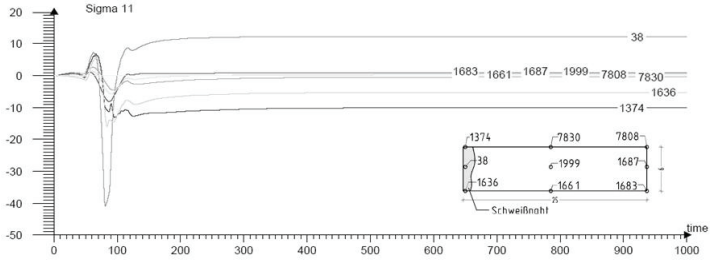

Figure 9: Time dependent axial stresses in direction orthogonal to the joint plane (time [s], stresses [N / mm^2])

In the final state, after complete cooling, a residual stress state arises, favourable to the silica that corresponds to the effect of the thermal tempering of toughened safety glass. On the top face of the weld compressive stresses of about σ_x = 10 N/mm^2 arise, in the centre of the weld tensile stresses of approximately σ_x = 13 N/mm^2 were calculated (figure 10).

Figure 10: Residual axial stresses orthogonal to the joint plane [N / mm^2]

"Viscous" Model (MAXWELL)

In this mechanical calculation, the previously described MAXWELL Model is applied. Geometrical parameters, as well as thermal factors, have not been modified compared to the STANDARD SOLID Model calculation. The residual axial stress distribution in cross direction of the plate perpendicular to the weld is shown in figure 11.

Figure 11: Residual axial stresses orthogonal to the joint plane [N / mm^2])

Here, the calculated residual axial stresses are σ_x = -6 N/mm^2 at the joint surface and σ_x = 14 N/mm^2 in the middle of the weld. The compressive stress field has a larger extension below the surface of the silica plate, caused by the increasing influence of viscoplastic behaviour in the STANDARD SOLID Model above the vitreous transition temperature.

LASER BEAM WELDING OF SILICA TUBES

In this example, the thermal and mechanical processes are analysed during a laser beam welding of butt-welded silica tubes. The welding parameters used in this case were derived from the proceeded test welding of silica plates. The numerical simulation will be carried out for a butt joint welding of silica tubes with 50 mm outer diameters and a wall-thickness of 5 mm. The welding velocity is 0,5 mm/s.

THERMAL PROCESSES

For the simulation of the energy input, two independent heat sources are used, similar to the welding of silica plates. A preheating laser beam with large beam radius and small maximum intensity causes an effective surface energy input of 178 W. A second laser beam with a small beam radius and high maximum intensity is led into the gap between the silica tubes. The effective power of the concentrated laser beam is 56 W. A reduction of the effects of energy losses from convection and radiation on the cylinder inner side are considered. The transient temperature field during the welding process is presented in figure 12. The increased laser power in comparison to the welding process of the silica plates leads to a continuous temperature field along the depth of the joint. The computed maximum temperature of T = 2500 °C is in this case below the pyrolysis temperature of SiO_2 of T = 2800 °C [Holleman-Wiberg 1995].

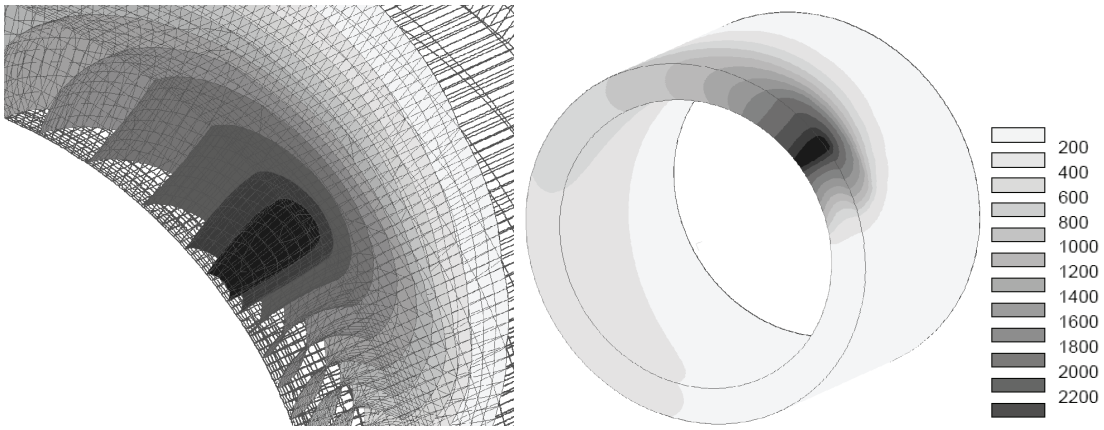

Figure 12: Temperature field in the joint during welding [°C]

MECHANICAL PROCESSES

Due to the high temperatures that occur during the welding process, the mechanical calculation was based to the model of MAXWELL. There is a strong geometrical influence, which is caused by the curvature of the tube. The residual axial stress running lengthwise along the tube is presented in figure 13.

The residual stress distribution shows a discontinuity in the field of joint rewelding at the end of the welding process. This irregularity should be moderated through adapted preheating procedures. One option is the delayed shutdown of the preheating laser beam. This reduces the temperature decreasing rate after finishing the welding process.

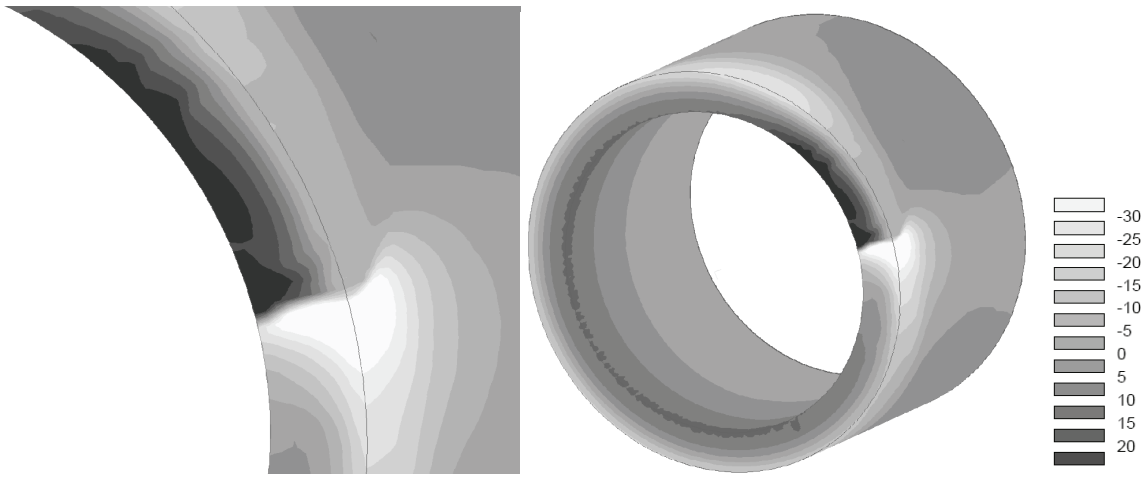

Figure 13: Residual axial stesses in tube lengthwise [N / mm^2])

CONCLUSIONS AND PROSPECTS

The use of the Finite-Element-Method allows the modelling of laser beam welding of silica. The application of the laser beam welding of silica requires an extensive adaptation of the material models used. The experimental tests showed that an optimisation of the process parameters (welding speed, laser power) is required in order to achieve an optimal welding result. Further research work is necessary related to the adaptation of this technology for the welding of other types of glasses. The next step will be the development of a welding procedure for borosilicate glass.

We would like to thank the Institute of Joining Technology and Materials Testing for their kind support and realisation of the experiments.

REFERENCES

Christensen, R. M. (1982), „Theory of viscoelasticity – An Introduction" Academic Press.

ESI-Group (2005), „SYSWELD 2005 Reference Manual".

Geotti-Bianchini, F., De Riu, L., Gagliardi, G., Guglielmi, M. und Pantano, CG. (1991), „New Interpretation of the IR reflectance spectra of SiO2-rich films on soda-lime glass", Glastechn. Berichte, Jg. 64, H. 8, S. 205-217.

Hohmann, R., Setzer, M. J. (1997), „Bauphysikalische Formeln und Tabellen", 3. Auflage, Werner-Verlag, Düsseldorf.

Holleman-Wiberg (1995), Lehrbuch der anorganischen Chemie, 34. Edition, 101. Auflage, Walter de Gruyter & Co., Berlin,

Radaj, D. (1999), „Schweißprozesssimulation, Grundlagen und Anwendung", DVS-Verlag, Düsseldorf.

Wächter, S., Kasch, S. und Müller, H. (2002), „Laserfügetechnologie für Glas und Keramik", DVS Berichte Band 211, S.87-95.